Highlighting a solid-like behavior in RTILs: tri-octylmethylammonium bis(trifluoromethanesulfonyl)imide TOMA-TFSI

Hakima Mendil-Jakani, Patrick Baroni, Laurence Noirez, Léa Chancelier, Gérard Gebel

THE JOURNAL OF PHYSICAL CHEMISTRY Letters

Letter

pubs.acs.org/JPCL

Highlighting a Solid-Like Behavior in RTILs: Trioctylmethylammonium Bis(trifluoromethanesulfonyl)imide TOMA-TFSI

Hakima Mendil-Jakani,*[,†] Patrick Baroni,[‡] Laurence Noirez,[‡] Léa Chancelier,[†] and Gérard Gebel[†]

[†]Structure et Propriétés d'Architectures Moléculaires, UMR 5819 SPRAM, (CEA-CNRS-UJF), CEA-Grenoble, 17 rue des Martyrs, 38054 Grenoble, Cedex 9, France

[‡]Laboratoire Léon Brillouin (CEA-CNRS), CEA-Saclay, 91191 Gif-sur-Yvette, France

ABSTRACT: Careful measurements of the dynamic response of the room -temperature ionic liquid (RTIL) trioctylmethylammonium bis(trifluoromethanesulfonyl)imide reveal that it exhibits actually a (low-frequency) solid-like response when solicited at the submillimeter scale with a low shear strain. The solid-like response is measured away from the glass transition (at around 100 °C above T_g), ruling out reminiscent transitional effects but suggesting that the dynamic properties of the RTIL are governed by long-range elastic intermolecular interactions.

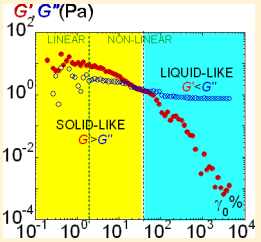

SECTION: Glasses, Colloids, Polymers, and Soft Matter

Room-temperature ionic liquids (RTILs) consist of a bulky organic cation and an organic or inorganic anion. Their remarkably low melting point is mainly due to the symmetry breaking structure of the cations.[1,2] Because they gather ionic, van der Waals, hydrogen bonding, and electrostatic interactions, their properties such as low vapor pressure,[3] good thermal and electrochemical stabilities,[4,5] low flash point,[6] and low flammability[7] make them unique. The infinite combination of anions and cations makes them also versatile. As a result, in less than a decade, RTILs have emerged as a new and alternative class of finely chemically tunable molecules suitable for a wide range of applications of advanced materials for catalysis, synthesis,[8,9] and lubrication.[10] They are also considered as potential electrolytes for very stringent specification electrochemical devices such as lithium batteries.[5,11,12] A better understanding of their physical properties is required to highlight the genuine potential of RTILs and the prospect for their future applications. A major drawback of RTILs, when used as electrolytes, is the often noticed high viscosity, which directly affects the conductivity.[5,13−15] Indeed, RTILs have shown aggregation in the liquid state,[16,17] which increases with the aliphatic group chain length.[16,18−23] Recently, it was shown, by measuring viscoelastic properties by ultrasonic spectroscopy, that is, in the MHz frequency range, that for long alkyl chains, RTILs no longer behave as Newtonian liquids but instead as interconnected structures.[24]

Herein, we report on the low-frequency dynamic relaxation behavior of a standard ionic liquid, the trioctylmethylammonium bis(trifluoromethanesulfonyl)imide, that is examined at large time scales (Hz) as close as possible to its equilibrium state. We reveal that this ionic liquid is not viscous but displays a *macroscopic solid-like* response even 100° C above the glass transition. This experimental result is obtained by analyzing the behavior of the ionic liquid to a low shear strain stress solicitation. In this experiment, the boundary conditions are optimized between the sample and the substrate, whereby the strain is applied and the stress is transmitted.[25−27]

We trust that the identification of solid-like correlations in RTILs, which imply collective elastic intermolecular interactions and long relaxation time scales,[26] will trigger new debates on the origin of their exceptional properties.

Material. The trioctylmethylammonium bis(trifluoromethanesulfonyl)imide (TOMA-TFSI) was purchased from IOLITEC and was used without further purification. It corresponds to the chemical formula shown in Figure 1. The glass transition temperature was measured by DSC and was −90 °C.

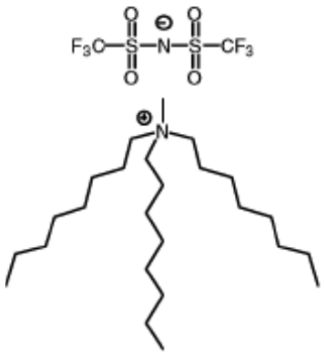

Figure 1. Chemical formula of TOMA-TFSI.

Received: September 10, 2013
Accepted: October 21, 2013

   dx.doi.org/10.1021/jz401938y | *J. Phys. Chem. Lett.* 2013, 4, 3775−3778

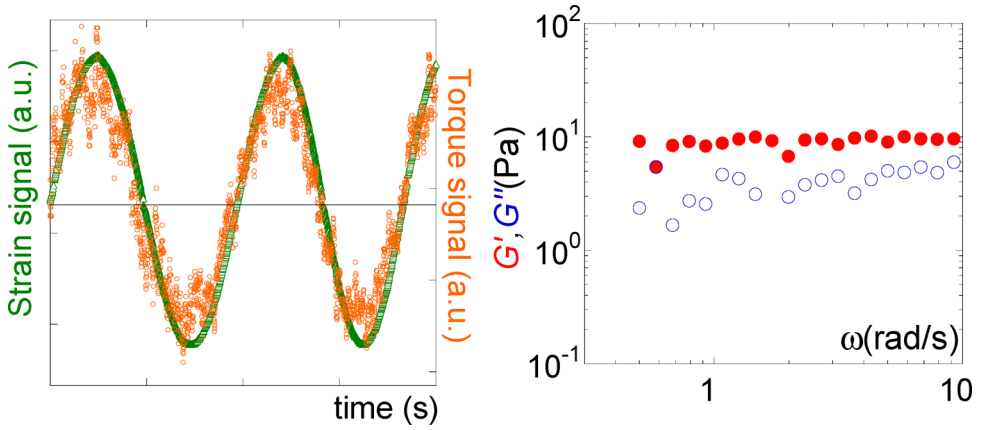

Figure 2. (Left) The input sinusoidal wave corresponds to the imposed strain amplitude (green △), and the ouptut sinusoidal wave corresponds to the measured torque (orange ○) at 22 °C, γ_0 = 1%, a 90 μm gap thickness, and a 40 mm diameter. (Right) Dynamic relaxation spectrum displaying the elastic $G'(\omega)$ (red ●) and viscous $G''(\omega)$ (blue ○) moduli of TOMA-TFSI at 22 °C, γ_0 = 1%, 90 μm gap thickness, and 40 mm diameter.

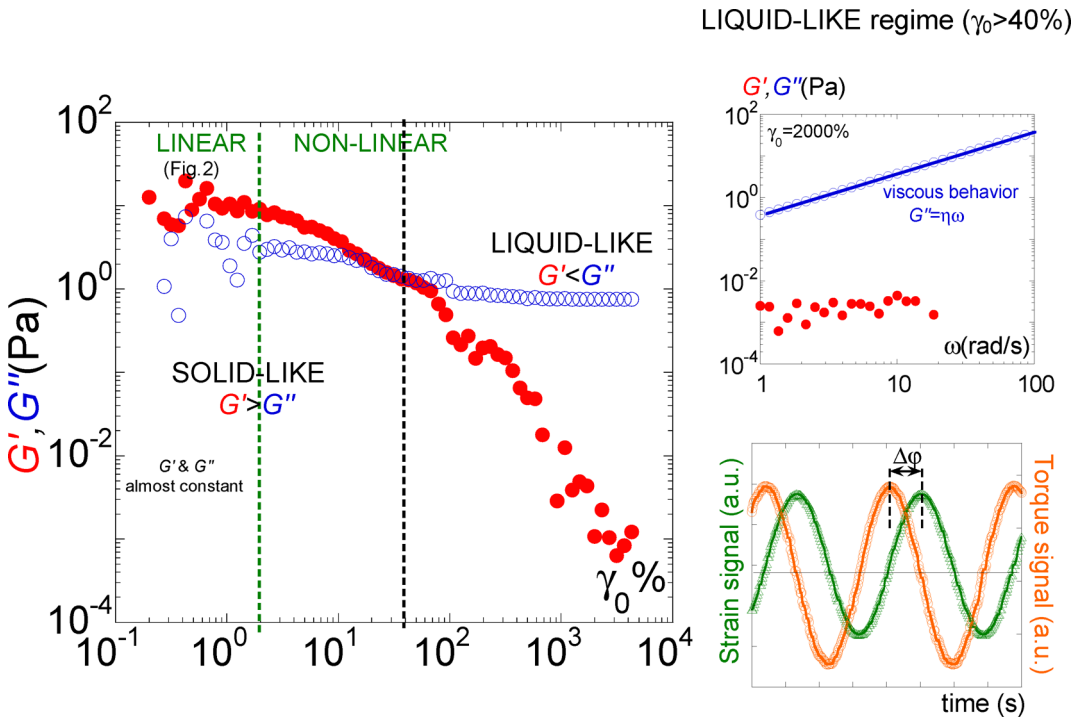

Figure 3. Elastic $G'(\omega)$ (red ●) and viscous $G''(\omega)$ (blue ○) moduli as a function of the strain amplitude at 1 rad/s and 90 μm gap thickness. The increasing level of deformation induces a transition from a solid-like (low strain amplitude) to a viscous-like behavior (large strain amplitude). The upper right satellite displays G' (red ●) and G'' (blue ○) at γ_0 = 2000%. The viscous modulus G'' obeys the ω-scale law, with the slope giving the viscosity. The viscous-like behavior is also illustrated by the out-of-phase torque (orange ○) signal versus the strain signal (green △) (lower right satellite). The phase shift $\Delta\varphi$ is close to 90°.

Dynamic Relaxation Measurements. Prior to experiment, TOMA-TFSI was vacuum-dried at room temperature to get rid of residual water and microbubbles that are detrimental for the quality of the measurement. The experiment was then performed under an argon atmosphere. The sample was placed in the gap between two coaxial disk-like fixtures (40 mm diameter). The zero gap was set by contact without the sample. The error was positive and less than 0.005 mm. The sample was probed at room temperature (22 °C, i.e., 112 °C above to the glass transition) in the low-frequency domain (typically from 0.1 up to 100 rad/s). We used small-amplitude oscillatory shear and improved boundary conditions between the sample and the substrate.[25] The strong interaction was satisfied by using alumina surfaces where the wetting of the sample was total. This allowed one to avoid the slipping at the liquid/substrate boundary to optimize the transmission of the imposed deformation from the surface to the sample.

A shear strain of amplitude γ_0 is transmitted to the sample by imposing a sinusoidal motion of variable frequency (ω) by contact with one disk. The second disk is immobile and coupled to a sensor to measure the stress transmitted by the sample. Simultaneously, a voltmeter measures the voltage of the motor imposing the oscillation, that is, the strain amplitude, while another voltmeter measures the voltage associated to the sensor, that is, the torque. This setup allows the simultaneous measurement of the shear strain and the shear stress signals.

dx.doi.org/10.1021/jz401938y | J. Phys. Chem. Lett. 2013, 4, 3775−3778

The dynamic relaxation profile is determined using the relationship $\sigma(\omega) = G_0\gamma_0 \sin(\omega t + \Delta\varphi)$, where $\sigma(\omega)$ is the shear stress, G_0 is the shear modulus, γ_0 is the strain amplitude, defined as the ratio of the displacement to the sample thickness, and $\Delta\varphi$ is the phase shift between the input and the output waves. This equation can be also expressed in terms of shear elastic (G') and viscous (G'') moduli, $\sigma(\omega) = \gamma_0(G'(\omega) \sin(\omega t) + G''(\omega) \cos(\omega t))$, with G' as the component in phase with the strain and G'' as the out-of-phase component.

Figure 2(left) displays the input sin strain wave and the output stress wave versus time of TOMA-TFSI at low strain amplitude (γ_0 = 1%), with a 90 μm gap thickness. Input and output sin waves are nearly superimposed. The ionic liquid responds instantaneously to the solicitation; this is the signature of a solid-like response.

The dynamic relaxation spectrum showing the frequency dependence of the elastic (G') and viscous (G'') moduli is displayed in Figure 2(right). The shear modulus G' is significantly higher than the viscous modulus G'', and both are weakly frequency-dependent in the explored frequency range. This typical solid-like response is in agreement with the in-phase stress output illustrated in Figure 2(left).

Strain Amplitude Effect. We analyze the effect of an increasing deformation rate on the solid-like response of TOMA-TFSI. Figure 3. displays the evolution of G' and G'' as a function of the strain amplitude γ_0 at ω = 1 rad/s.

Figure 3 shows that up to γ_0 = 2%, G' is higher than G'', almost independently of the strain amplitude defining the linear domain of the solid-like response. Above γ_0 = 2%, the viscoelastic response is nonlinear; G' becomes strongly strain-dependent, while G'' is much less affected. The sample exhibits a predominant elastic response up to $\gamma_0 \approx$ 40%. Above γ_0 = 40%, G'' becomes significantly higher than G'; the viscous contribution becomes predominant for high strain amplitude. The strong lowering of the elastic contribution with the strain amplitude gives rise to a flow behavior, as shown in the upper right satellite of Figure 3. It follows that G'' obeys the conventional ω-scaling behavior with a slope of η = 380 mPa·s, which is in agreement with the tabulated values for similar RTILs.[10,19] The lower right satellite displays the corresponding input sin strain wave and the output torque wave, which are, as expected, significantly out of phase. The 90° phase shift at high strain amplitudes indicates the loss of the elastic component and thus the recovery of a viscous behavior. Therefore, the ionic liquid displays a flow behavior at high strain amplitude only; it is plastic, characterized by a stress/strain threshold.

Sample Thickness Effect. Figure 4 displays the evolution of the low-frequency shear elasticity measured at low strain amplitude as a function of the sample thickness. $\langle G' \rangle$ is the value of the elastic modulus G' averaged on the frequency plateau (0.2 up to 10 rad/s). The solid-like behavior is reinforced at low sample thicknesses and collapses by increasing the sample gap. For larger thicknesses, the standard viscous behavior is recovered. The thickness dependence of the moduli has been already reported by different authors in different liquids and complex fluids from glass-formers[27−29] to liquid water.[30] Similar multiscale effects are well-known for foams,[31] clays, or cement pastes[32] and might be here related to a scaling effect due to a loss of the correlation range of intermolecular interactions.

The strength of the elasticity seems to be linked to the nature of the intermolecular interactions (van der Waals, ionic, Coulomb interactions, H-bond), which is a function of the sample chemistry and molecular architecture.[26] Indeed, the

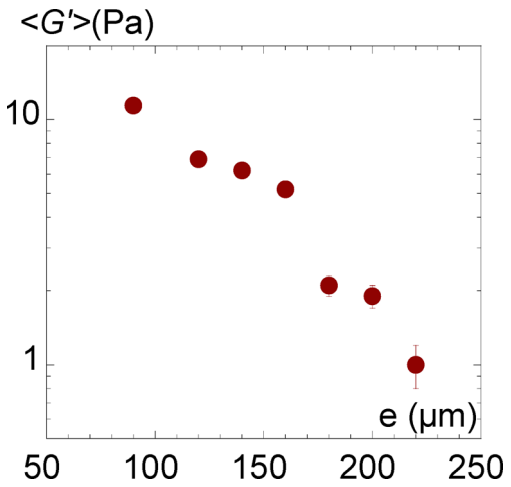

Figure 4. Average value $\langle G' \rangle$ of the elastic modulus G' as a function of the sample thickness. Above 220 μm, the elastic response is no longer measurable; the viscous response is recovered.

elasticities measured for polypropylene glycol, *ortho*-terphenyl, glycerol, water, and the RTIL 1-ethyl-3-methylimidazolium bis(trifluoromethylsulfonyl)imide [emim][Tf2N] were, respectively, 250, 200, 40, 2, and 1 Pa. The elasticity measured for [emim][Tf2N] was about 10 times lower than that for TOMA-TFSI. The stronger TOMA-TFSI elasticity is explained by the strongest van der Waals intermolecular interactions involved for TOMA-TFSI, whose cation is grafted by three long alkyls chains.

Solid-like shear elasticity has been highlighted at the submillimetric scale by low-frequency mechanical solicitation in the liquid phase (at room temperature) of the TOMA-TFSI. This macroscopic property can be revealed provided that the liquid is solicited with small strain amplitudes and is strongly anchored on the substrate. Both conditions are required to enable the transmission of mechanical stress to the sample and to keep the liquid close to a nonperturbed state (linear conditions). We demonstrate that the ionic liquid displays a standard flow behavior under perturbative conditions (obtained by applying large strain amplitude oscillation) or at large sample thicknesses. These particular conditions might explain why the solid-like behavior is hardly detectable in conventional experimental conditions (i.e., for gap thicknesses on the order of 1 mm or more). In the present study, the thicknesses probed (from 60 up to 220 μm) exceed greatly the molecular scale, indicating that the shear elasticity is a macroscopic property that cannot be related to surface-induced effects such as liquid crystallinity (the coherence length in the isotropic phase of liquid crystals is around 200 Å[29]).

The finite shear elasticity of RTILs[26] shows that these molecular liquids behave as yield stress fluids that flow up to a critical shear strain/stress. Because the long-range elastic correlations are related to long relaxation time scales, the role of the shear elasticity has to be considered for a better understanding of odd properties such as the non-Arrhenius evolutions of the viscosity and conductivity with temperature,[5] the deviation from the Nernst−Einstein equation and the variation of the Walden product recently ascribed to the variation in the high-frequency shear modulus with lengthening alkyl chain.[33] The solid-like behavior, showing that the aggregation state is not restricted to several molecular lengths but extended to the macroscopic scale, calls for further

dx.doi.org/10.1021/jz401938y | J. Phys. Chem. Lett. 2013, 4, 3775−3778

theoretical developments and simulations, taking into account the wide panel of length and time scales. Therein, it is interesting to emphasize that the ability of RTILs to form strongly interconnected molecular interactions is evidenced with at least 6 orders of magnitude separating the dynamics probed by ultrasonic spectroscopy (MHz range)[24] from the dynamic measurements reported here (Hz range).

AUTHOR INFORMATION

Corresponding Author

*E-mail: hakima.mendil-jakani@cea.fr. Tel: +33 4 38 78 91 71. Fax: +33 4 38 78 56 91.

Notes

The authors declare no competing financial interest.

REFERENCES

(1) Holbrey, J. D.; Seddon, K. R. The Phase Behaviour of 1-Alkyl-3-methylimidazolium Tetrafluoroborates; Ionic Liquids and Ionic Liquid Crystals. *J. Chem. Soc., Dalton Trans.* **1999**, *13*, 2133−2139.

(2) Dean, P. M.; Pringle, J. M.; MacFarlane, D. R. Structural Analysis of Low Melting Organic Salts: Perspectives on Ionic Liquids. *Phys. Chem. Chem. Phys.* **2010**, *12*, 9144−9153.

(3) Paulechka, Y. U.; Kabo, G. J.; Blokhin, A. V.; Vydrov, O. A.; Magee, J. W.; Frenkel, M. Thermodynamic Properties of 1-Butyl-3-methylimidazolium Hexafluorophosphate in the Ideal Gas State. *J. Chem. Eng. Data* **2003**, *48*, 457−462.

(4) Garcia, B.; Lavallee, S.; Perron, G.; Michot, C.; Armand, M. Room Temperature Molten Salts as Lithium Battery Electrolyte. *Electrochim. Acta* **2004**, *49*, 4583−4588.

(5) Lewandowski, A.; Swiderska-Mocek, A. Ionic Liquids as Electrolytes for Li-Ion Batteries—An Overview of Electrochemical Studies. *J. Power Sources* **2009**, *194*, 601−609.

(6) Liaw, H.-J.; Chen, C.-C.; Chen, Y.-C.; Chen, J.-R.; Huang, S.-K.; Liu, S.-N. Relationship Between Flash Point of Ionic Liquids and Their Thermal Decomposition. *Green Chem.* **2012**, *14*, 2001−2008.

(7) Fox, D. M.; Gilman, J. W.; Morgan, A. B.; Shields, J. R.; Maupin, P. H.; Lyon, R. E.; De Long, H. C.; Trulove, P. C. Flammability and Thermal Analysis Characterization of Imidazolium-Based Ionic Liquids. *Ind. Eng. Chem. Res.* **2008**, *47*, 6327−6332.

(8) Wasserscheid, P.; Welton, T. *Ionic Liquids in Synthesis*; Wiley-VCH Verlag GmbH & Co. KGaA: Weinheim, Germany; 2002.

(9) Welton, T. Ionic Liquids in Catalysis. *Coord. Chem. Rev.* **2004**, *248*, 2459−2477.

(10) Karna, M.; Lahtinen, M.; Kujala, A.; Hakkarainen, P. L.; Valkonen, J. Properties of New Low Melting Point Quaternary Ammonium Salts with Bis(trifluoromethanesulfonyl)imide anion. *J. Mol. Struct.* **2010**, *983*, 82−92.

(11) Armand, M.; Tarascon, J. M. Building Better Batteries. *Nature* **2008**, *451*, 652−657.

(12) Armand, M.; Endres, F.; MacFarlane, D. R.; Ohno, H.; Scrosati, B. Ionic-Liquid Materials for the Electrochemical Challenges of the Future. *Nat. Mater.* **2009**, *8*, 621−629.

(13) Tokuda, H.; Hayamizu, K.; Ishii, K.; Susan, M. A. B. H.; Watanabe, M. Physicochemical Properties and Structures of Room Temperature Ionic Liquids. 2. Variation of Alkyl Chain Length in Imidazolium Cation. *J. Phys. Chem. B* **2005**, *109*, 6103−6110.

(14) Triolo, A.; Russina, O.; Bleif, H. J.; Di Cola, E. Nanoscale Segregation in Room Temperature Ionic Liquids. *J. Phys. Chem. B* **2007**, *111*, 4641−4644.

(15) Allen, J. J.; Schneider, Y.; Kail, B. W.; Luebke, D. R.; Nulwala, H.; Damodaran, K. Nuclear Spin Relaxation and Molecular Interactions of a Novel Triazolium-Based Ionic Liquid. *J. Phys. Chem. B* **2013**, *117*, 3877−3883.

(16) Le, M. L. P.; Alloin, F.; Strobel, P.; Lepretre, J. C.; del Valle, C. P.; Judeinstein, P. Structure−Properties Relationships of Lithium Electrolytes Based on Ionic Liquid. *J. Phys. Chem. B* **2010**, *114*, 894−903.

(17) Hardacre, C.; Holbrey, J. D.; Mullan, C. L.; Youngs, T. G. A.; Bowron, D. T. Small Angle Neutron Scattering from 1-Alkyl-3-methylimidazolium Hexafluorophosphate Ionic Liquids ($[C_n mim][PF_6]$, n = 4, 6, and 8. *J. Chem. Phys.* **2010**, *133*, 074510/1−074510/7.

(18) Zhao, Y.; Gao, S. J.; Wang, J. J.; Tang, J. M. Aggregation of Ionic Liquids $[C_n mim]Br$ (n = 4, 6, 8, 10, 12) in D_2O: A NMR Study. *J. Phys. Chem. B* **2008**, *112*, 2031−2039.

(19) Kunze, M.; Jeong, S.; Paillard, E.; Schonhoff, M.; Winter, M.; Passerini, S. New Insights to Self-Aggregation in Ionic Liquid Electrolytes for High-Energy Electrochemical Devices. *Adv. Energy Mater.* **2011**, *1*, 274−281.

(20) Russina, O.; Triolo, A.; Gontrani, L.; Caminiti, R. Mesoscopic Structural Heterogeneities in Room-Temperature Ionic Liquids. *J. Phys. Chem. Lett.* **2012**, *3*, 27−33.

(21) Dorbritz, S.; Ruth, W.; Kragl, U. Investigation on Aggregate Formation of Ionic Liquids. *Adv. Synth. Catal.* **2005**, *347*, 1273−1279.

(22) Hayamizu, K.; Tsuzuki, S.; Seki, S.; Umebayashi, Y. Nuclear Magnetic Resonance Studies on the Rotational and Translational Motions of Ionic Liquids Composed of 1-Ethyl-3-methylimidazolium Cation and Bis(trifluoromethanesulfonyl)amide and Bis-(fluorosulfonyl)amide Anions and Their Binary Systems Including Lithium Salts. *J. Chem. Phys.* **2011**, *135*, 084505/1−084505/11.

(23) Noda, A.; Hayamizu, K.; Watanabe, M. Pulsed-Gradient Spin−Echo ^1H and ^{19}F NMR Ionic Diffusion Coefficient, Viscosity, and Ionic Conductivity of Non-Chloroaluminate Room-Temperature Ionic Liquids. *J. Phys. Chem. B* **2001**, *105*, 4603−4610.

(24) Makino, W.; Kishikawa, R.; Mizoshiri, M.; Takeda, S.; Yao, M. Viscoelastic Properties of Room Temperature Ionic Liquids. *J. Chem. Phys.* **2008**, *129*, 104510/1−104510/7.

(25) Baroni, P.; Mendil, H.; Noirez, L. *Procédé & Dispositif pour la Détermination d'au moins une Propriété Dynamique d'un Fluide ou d'un Solide Déformable*. Patent n°0510988, 2005.

(26) Noirez, L.; Baroni, P.; Cao, H. J. Identification of Shear Elasticity at Low Frequency in Liquid n-Heptadecane, Liquid Water and RT-Ionic Liquids [Emim][Tf2N]. *J. Mol. Liq.* **2012**, *176*, 71−75.

(27) Martinoty, P.; Collin, D. Dynamic Macroscopic Heterogeneities in a Fexible Linear Polymer Melt. *Physica A* **2002**, *320*, 235−248.

(28) Mendil, H.; Baroni, P.; Noirez, L. Solid-Like Rheological Response of Non-Entangled Polymers in the Molten State. *Eur. Phys. J. E* **2006**, *19*, 77−85.

(29) Noirez, L.; Mendil-Jakani, H.; Baroni, P. Identification of Finite Shear-Elasticity in the Liquid State of Molecular and Polymeric Glass-Formers. *Philos. Mag.* **2011**, *91*, 1977−1986.

(30) Noirez, L.; Baroni, P. Identification of a Low-Frequency Elastic Behaviour in Liquid Water. *J. Phys.: Condens. Matter* **2012**, *24*, 372101/1−372101/6.

(31) Heller, J. P.; Kuntamukkula, M. S. Critical-Review of the Foam Rheology Literature. *Ind. Eng. Chem. Res.* **1987**, *26*, 318−325.

(32) Bazant, Z. P. *Scaling of Structural Strengths*; Hermes Penton Science: London; 2002.

(33) Yamaguchi, T.; Nakahara, E.; Sueda, K.; Koda, S. Interpretation of the Variation of the Walden Product of Ionic Liquids with Different Alkyl Chain Lengths in Terms of Relaxation Spectra. *J. Phys. Chem. B* **2013**, *117*, 4121−4126.